IEEE Access
Multidisciplinary | Rapid Review | Open Access Journal

Received 10 April 2023, accepted 16 April 2023, date of publication 25 April 2023, date of current version 3 May 2023.

Digital Object Identifier 10.1109/ACCESS.2023.3270310

RESEARCH ARTICLE

Drivers' Workload Electroencephalogram Characteristics in Cognitive Tasks Based on Improved Multiscale Sample Entropy

RUIWEI LIU[1], SHOUMING QI[2,3], SIQI HAO[4], GUAN LIAN[5], YINGTONG LI[4], AND HAIHUA YANG[6]

[1]School of Naval Architecture and Ocean Engineering, Guangzhou Maritime University, Guangzhou 510725, China
[2]School of Civil and Environmental Engineering, Harbin Institute of Technology at Shenzhen, Shenzhen, Guangdong 518055, China
[3]Shenzhen Urban Public Safety and Technology Institute, Shenzhen, Guangdong 518000, China
[4]Department of Ports and Shipping Management, Guangzhou Maritime University, Guangzhou 510700, China
[5]Guangxi Key Laboratory of ITS, Guilin University of Electronic Technology, Guilin 541000, China
[6]China Construction Infrastructure Corporation Ltd., Beijing 100029, China

Corresponding author: Shouming Qi (shouming1991@163.com)

This work was supported in part by the National Natural Science Foundation of China under Grant 52105011 and Grant 52102410, in part by the Guangxi Science and Technology Base and Talent Special Project under Grant AD19245021, in part by the Young Innovative Talents Project of Guangdong Province under Grant 2021KQNCX071 and Grant 2021KQNCX073, in part by the Tertiary Education Scientific Research Project of Guangzhou Municipal Education Bureau under Grant 202235334, and in part by the 2023 Basic Research Plan Program of Guangzhou under Grant SL SL2023A04J00685 and SL2023A04J00686.

ABSTRACT Cognitive workload is an internal factor that can be influenced by external factors. When drivers are distracted by these internal and external influences, their ability to drive safely can be compromised. Electroencephalogram (EEG) is a non-invasive neuroimaging technique that measures the electrical activity of the brain. and it can provide information about brain activity related to various cognitive and motor functions. In this study, on-road driving experiments were conducted to investigate the EEG characteristics of drivers under different levels of cognitive workload generated through mathematical calculations with varying difficulties. The collected EEG signals were processed using continuous wavelet transform to decompose them into delta, theta, alpha, beta, and gamma waveforms. Numerical values and power spectral characteristics of each waveband in the left and right frontal regions of the driver were then analyzed. Furthermore, the study utilized an improved multiscale sample entropy algorithm to analyze the EEG entropy characteristics of drivers in different states. The results indicate that under different degrees of cognitive workload, the amplitude of delta, theta, and alpha waves decreased, while beta and gamma waves showed significant changes. The improved multiscale sample entropy algorithm provided a more objective assessment of changes in entropy across different wavebands and stages, with smaller entropy fluctuation ranges and more accurate complexity changes. Overall, this research provides valuable insights into the characteristics of drivers under cognitive workload, contributing to the analysis of human factors in driving safety. These findings can inform the development of strategies to mitigate the adverse effects of cognitive workload on driving performance and enhance overall road safety.

INDEX TERMS Cognitive workload, EEG characteristics, continuous wavelet transform, power spectrum characteristics, improved multiscale sample entropy.

I. INTRODUCTION

In recent years, people's travel patterns have undergone great changes, and traffic accidents have continued to increase. The main causes of global traffic accidents are drunk driving, fatigue driving and distracted driving [1]. How to make intelligent auxiliary systems better understand the characteristics of drivers and ensure personalised service has become a hot issue in traffic safety research. Electroencephalogram (EEG) signals are regarded as an objective indicator of drivers'

The associate editor coordinating the review of this manuscript and approving it for publication was Shovan Barma.

activities and have attracted much attention. In the process of driving, drivers are usually interfered by various external factors, such as cognitive workload, which directly affect the decision-making of the driver's brain and have a significant impact on driving safety. The exploration of cognitive workload has always been a hot spot in the field of neuroscience. Studying cognitive behaviour with changes in EEG signals can improve driving safety, provide a theoretical basis for the development of driving assistance systems and have more practical application value.

The brain wave was first detected by Hans Berger in 1924, and the brain activity is called electromyogram [2]. Subsequently, an increasing number of scientists are conducting research on human EEG in different fields, analysing its generation mechanism and changing rules [3]. The electroencephalogram, represented by waves, contains a great deal of information about disease and physiology. The frequency of human brain electrical signals is usually in the range of 0.5–50 Hz, and the amplitude of brain electrical signals is usually 5–200 μV. According to the different frequencies, EEG signals are usually divided into five frequency bands: delta, theta, alpha, beta and gamma waves. Different waveforms can reflect the different mental states of the brain [4]. Many studies have shown that mental arithmetic has an effect on electrical activity in the brain. Cohen et al. found that the prefrontal cortex is related to the data extraction work of calculation, and the top area is responsible for calculation [5]. Kong et al. studied the impact of the cognitive workload of varying difficulties on the brain potential and found that one can be more easily distracted when calculating high-difficulty tasks than low-difficulty tasks [6]. Kou et al. found that mental computation has a greater impact on the frontal and parietal lobes of the brain [7]. Aydin et al. found that the temporal lobe region responds to auditory stimuli, while the frontal lobe region simultaneously integrates auditory tasks [8].

Brain waves are closely related to the state of the driver. Some studies are based on EEG activity indicators under normal conditions. An analysis of the changes in EEG under different conditions found that the activity of delta and theta waves is most closely related to driving fatigue [9], [10]. The activity level of theta wave will increase with increasing fatigue [11], while the activity of beta wave will decrease under driving fatigue [12], [13]. On the basis of a study on changes in a certain waveform activity, the ratio of fast waves and slow waves in different frequency bands is often used to reflect the brain's electrical activity—for example, theta/beta; theta/(alpha + beta); (theta + alpha)/beta; (theta + alpha)/(alpha + beta) and many other forms [14], [15], [17]. The four equations listed all include theta activity as slow-wave activity and beta as fast-wave activity. Many cognitive tasks are interfering tasks, such as mathematical problem calculation, N-back or decision-making tasks. Lin et al. designed experiments on math problem calculation interference to produce cognitive distraction and found that the power of the theta wave and beta wave in the frontal area of the brain increases during distraction, and the power increase of the theta wave will reflect the degree of interference during actual driving [18]. Borghini et al. analysed the influence of mental workload on brain activity through EEG signals and found that with the deepening of mental workload, the energy of the theta wave increased, and the energy of the alpha wave decreased [19].

With the development of digital technology, more complex system methods are used to quantify brain functions. Entropy is the most commonly used method. It can measure the complexity of the brain and the network characteristic parameters for studying brain functions. The entropy of a single discrete random variable is a measure of its uncertainty, which can characterise the degree of randomness of the random variable. Based on the entropy parameter, it can reflect the orderly changes of complex systems and point out the development trend of the system, thus being used in the assessment of brain function status [20]. The approximate entropy was proposed so that its algorithm can be calculated with a small amount of data and applied to the analysis of physiological signals [21]. The approximate entropy algorithm was improved to obtain sample entropy, which further expanded the application scope of entropy theory in physiological data analysis [22]. A multi-scale sample entropy algorithm was proposed, which can measure the complexity of a finite long-time sequence [23]. Currently, it is widely used in the analysis of biological signals. Many scholars have also proved that evaluating the time correlation on different scales has an important role in studying the characteristics of brain electrical signals [24], [25], [26], [27], [28]. Many scholars have also reconstructed the multi-scale entropy method through research. For example, to reflect the existence of high-frequency components of physiological signals, Ahmed et al. combined empirical mode decomposition with multi-scale and proposed multivariate sample entropy, which can be applied to stable data testing [29]. Hu et al. proposed the adaptive multiscale entropy method, which improved the algorithm in the frequency domain [30]. Costa et al. improved their own algorithm and proposed to use variance instead of average to reconstruct time series on various scales [31]. Khanna A et al. proposed the idea of non-uniform segmentation based on spatial trends, which can be divided into several non-uniform segments according to the hidden space information of the time series to improve the accuracy of the data [32].

The current research results indicate that many achievements have been made in the study of EEG signal decomposition and cognitive workload on human behaviour. For EEG frequency, alpha and beta waveforms are mostly the main research objects, but few scholars study the characteristics of gamma wave (which is highly related to people's learning and cognitive behaviour). As for research on the influence of cognitive workload generated by mathematical calculations on EEG, it mainly involves laboratory instrument tests,

mostly for psychological or medical purposes. As a group that is prone to cognitive load, drivers have many mysteries in their brain electrical properties. Most related studies focus on driving fatigue characteristics, and a few scholars implement driving simulations to study the impact of cognitive workload on drivers' EEG.

Therefore, this paper will conduct on-road driving experiments to make drivers generate cognitive distraction workload by calculating math problems or varying difficulties and analysing the collected EEG data to study the behaviour characteristics of drivers. The EEG signal decomposed into five different bands of 0.5–50 HZ will be analysed through continuous wavelet transform, and the waveform will be reorganised to achieve denoising. The effects of different cognitive distraction workloads on drivers were analysed by comparing the left and right brains. The fine-grain method requires more time in the calculation process; thus, the multi-scale entropy of the coarse-grain method is used more frequently. However, the problem of short sequence and information loss is prone to occurring. Improving the coarse-grain method and adopting the method of moving delay value can reduce the fluctuation and dispersion degree between scales and avoid important information loss. This approach is used to analyse the EEG characteristics of drivers in different cognitive distractions. In this paper, the influence of different cognitive distraction workloads on drivers' brain electricity is studied, which can be used to analyse drivers' characteristics in the field of human factors and make a beneficial contribution to the improvement of driving safety.

II. EXPERIMENTAL PROCESS

A. PARTICIPANTS

Many studies have proved that small samples can also be used in driver characteristic tests. Usually, the number of samples is greater than 6 to be effective [33], [34], [35]. Twenty individuals (10 males and 10 females) with a mean age of 34 years old (SD = 8.65, age distribution ranges from 25 to 55 years) were recruited from the university community. They have a mean driving experience of 7 years (SD = 6.96). The purpose was to select a group of people who were representatives of the drivers in the urban traffic environment. To ensure driving safety, they need to be familiar with the local traffic environment and to have driving licenses. According to the preliminary screening survey, they had 20/20 or corrected-to-normal vision with no mobility impairments. They were not allowed to drink or smoke the day before the experiment and remained healthy.

B. APPARATUS AND EXPERIMENTAL ROUTES

The experiment involved one conventional vehicle (2017 SAGITAR 1.6T) with a human driver controlling the throttle, brake and steering. To capture data related to the driver's actions and status in real time, the vehicle was equipped with a laser ranging sensor (ranging scope of 0.5–200 m, ranging accuracy of ±0.5–1 m, measuring frequency of 10–50 HZ), radar rangefinder and four synchronised cameras (recording the front and rear of the vehicle, the driver's face and on-board operation video). The driver wore an EEG collection device (NeuroOne EEG, with 21 sampling channels) while driving. The drivers operate in accordance with their own daily driving behaviours, thereby collecting their natural driving behaviour in a real environment.

The starting point of the experimental route was the intersection of Songpu Bridge and Zhongyuan Avenue (Harbin, China), and the ending point was the intersection of Zhongyuan Avenue and Xiang'an North Avenue, with a total length of 10 kilometres. The road has six lanes in both directions, separated by a central dividing belt and traffic in the opposite direction. The experimental route was in good condition, and the driver had clear vision. The test time was 9:30–11:00 in the morning or 2:30–4:00 in the afternoon on weekdays. All testers conducted experiments on the same line. No collision accident occurred in all experiments.

C. EXPERIMENTAL PROCESS

1) The staff introduced the driving test process to the participants and asked for their personal information. After confirming that participants are qualified, the staff helped them wear the device. 2) The staff guided the driver to the test vehicle, turned on all the test equipment and completed the calibration and synchronisation of the equipment. In addition to the participant, the vehicle had two staff members; one was responsible for adjusting the experimental equipment, and the other was responsible for issuing the instructions required for the experiment. 3) Once the preparations were complete, the participants were allowed to drive in a safe area for approximately 15 minutes to accommodate the vehicle and the collection device. 4) The participants drove into the designated test route and started driving. The staff marked the starting point and began to record data. Unless there was a safety hazard, the participants had to cooperate with the instructions required to complete the experiment under the guidance of staff. 5) On certain road sections, the driver performed cognitive workload tasks while maintaining the main driving tasks. They completed the corresponding mathematical calculations according to the experimental design settings. If a dangerous situation occurred, then the driver had the right to choose to terminate the task. 6) After reaching the ending point, the staff marked the camera and ended the recording of the experimental instruments. After turning off all the instruments, they led the driver to a designated place to rest and removed the device for him/her. 7) The participants completed the final questionnaire and received a test reward (200 RMB). The staff then copied and archived the test data.

The cognitive load task usually adopts N-back, mathematical problem calculation, etc. This experiment conduct listening and calculating mathematical problems to reflect the cognitive workload. According to the difficulty of the questions, they were divided into three levels: simple, general and complex. At the same time, the cognitive load of mild, moderate and high levels was defined when drivers distracted with

different difficulties of problems, as illustrated in **Table 1**. Besides, to ensure the effectiveness of on-road experiment, this experimental scheme, the number of questions, and time limit of answering were repeatedly tested and determined in the indoor experiment. All the participants have a good mathematical foundation. Each participant needs to complete the experiments twice.

TABLE 1. Description of different cognitive workload tasks.

Difficulty of question	Cognitive work load	Types of distraction tasks	Example of question	Quantity of question	Time limit for answer(s)
simple	mild	non carry addition of double-digit positive number	22+24 =	3	6
		non carry subtraction of double-digit positive number	27-13=	2	
general	moderate	carry addition of double-digit positive number	18+15 =	2	10
		carry subtraction of double-digit positive number	52-19=	1	
complex	high	subtraction of double-digit negative number	15-38=	1	15
		continuous addition of double-digit positive number	14+25 +33=	1	

III. METHODOLOGY

A. CONTINUOUS WAVELET TRANSFORM

The original EEG signals are filtered using a 50Hz notch filter and sampled at a rate of 256Hz. All electrodes are referenced to the average electrode. To increase confidence in the obtained data, the raw EEG signals are divided into non-overlapping windows of 5 seconds and irrelevant electrodes are removed based on the sample. The impact of different frequency bands on drivers varies due to their distinct characteristics. Therefore, a certain method is needed to decompose waves of different frequencies. The use of wavelet transforms can better reveal the frequency features of EEG.

The time-frequency window of the wavelet transforms changes with the signal components to be analysed. The expansion and translation of the window are determined by the expansion factor and the translation factor. Wavelet transform mainly has the advantage of reducing the correlation between different features by selecting suitable filters. Two types of wavelet transform exist: continuous wavelet transform (CWT) and discrete wavelet transform. In this paper, CWT is used.

A real signal with limited energy is assumed if its Fourier transform satisfies (1)

$$C_\psi = \int_{-\infty}^{+\infty} \frac{\left|\hat{\psi}(\omega)\right|^2}{|\omega|} d\omega < +\infty \tag{1}$$

$\psi(t)$ is the basic wavelet (mother wavelet), and C_ψ is a permissible constant.

$\hat{\psi}(\omega)$ is the Fourier transform of $\psi(t)$, specifically shown in (2). The corresponding inverse Fourier transform is shown in (3). w is the angular frequency.

$$\hat{\psi}(\omega) = \int_{-\infty}^{+\infty} \psi(t) e^{-j\omega t} dt \tag{2}$$

$$\psi(t) = \frac{1}{2\pi} \int_{-\infty}^{+\infty} \hat{\psi}(\omega) e^{j\omega t} d\omega \tag{3}$$

By expanding and translating the basic wavelet, we obtain (4)

$$\psi_{s,\tau}(t) = \frac{1}{\sqrt{s}} \psi\left(\frac{t-\tau}{s}\right), \quad s, \tau \in R, s > 0 \tag{4}$$

where $\psi_{s,\tau}(t)$ is the wavelet basic function, s is the scale factor and τ is the translation factor.

$\psi_{s,\tau}(t)$ is determined by parameter s, and s controls the expansion and contraction of the wavelet function, which corresponds to frequency (inversely proportional), τ controls the translation of the wavelet function, which corresponds to time. The parameters s and τ are taken continuously; thus, $\psi_{s,\tau}(t)$ is a continuous wavelet basis function. The function $f(t)$ with finite energy in any $L^2(R)$ space is transformed with the function $\psi_{s,\tau}(t)$ as the integral core. This is called CWT, as shown in (5).

$$\begin{aligned} W_\psi(s,\tau) &= \left\langle f(t), \psi_{s,\tau}(t) \right\rangle \\ &= \int_R f(t)\psi_{s,\tau}(t)dt = \frac{1}{\sqrt{s}} \int_R f(t)\psi^*\left(\frac{t-\tau}{s}\right) dt \end{aligned} \tag{5}$$

where $W_\psi(s,\tau)$ is the wavelet transform coefficient; $\psi^*(t)$ is the complex conjugate function, which satisfies oscillating, time-frequency localisation; and $s \neq 0$, t and τ are continuous variables.

The continuous wavelet inverse transformation or the original signal reconstruction of $f(t)$ is shown in (6).

$$f(t) = \frac{1}{C_\psi} \int_0^{+\infty} \int_{-\infty}^{+\infty} W_\psi(s,\tau) \frac{\psi_{s,\tau}(t)}{s^2} ds d\tau \tag{6}$$

It is analysed by the Morlet basis function, a single-frequency sine function under a Gaussian envelope and composed of a complex trigonometric function multiplied by an exponential decay function. It is characterised by no

scaling function itself and a non-orthogonal decomposition. The Morlet basis function is expressed as (7)

$$\psi(t) = e^{-\frac{1}{2}t^2}\cos(2\pi f_0 t) \tag{7}$$

where f_0 is the centre frequency.

The collected brainwave data were processed, and the delta, theta, alpha, beta and gamma brain waves of different frequency bands were obtained through continuous wavelet decomposition, with a sample shown in **Fig. 1**. The waves of these five frequency bands were reconstructed by wavelet, and the new waveform was obtained, as shown in **Fig. 2**.

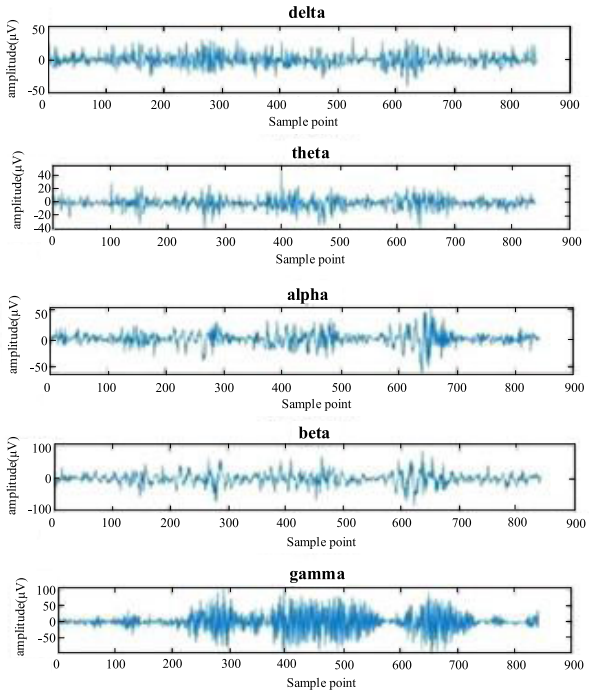

FIGURE 1. Schematic of wavelet transforms.

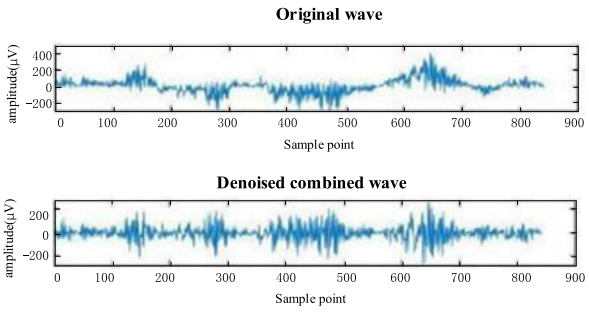

FIGURE 2. Schematic of denoised combined wave.

As can be seen in **Fig. 2**, compared with the original brain wave, the recombined brain wave with a frequency of 0.5–50 Hz has an obvious effect of denoising.

B. IMPROVED MULTI-SCALE SAMPLE ENTROPY

Entropy is the most commonly used method to measure the complexity of the brain. Based on entropy parameters, changes in the orderliness of complex systems can be reflected, and the development trend of the system can be studied. Therefore, entropy theory can be used for the evaluation of brain functional states. Sample entropy is a common used method in EEG signal analysis. Its main feature is that its calculation process does not depend on the length of data, which helps to improve the real-time performance of the system and is insensitive to lost data. The biggest difference between sample entropy and approximate entropy is that self template matching is not performed, and self matching is not included in statistics. The lower the sample entropy, the higher the self similarity of the sequence, and the greater the entropy, the more complex the sequence.

In the field of EEG research, the methodology has gradually transitioned from sample entropy to multi-scale sample entropy. Multi-scale sample entropy can measure the probability of generating new patterns in a time series. A high entropy value corresponds to a great probability of generating new patterns and a complex sequence. It requires less data, has better anti-noise and anti-interference capabilities, and can analyse and determine signals, including random signals. The algorithm steps are as follows:

An N-dimensional time series $X_N = \{x_1, x_2, x_3, \cdots, x_N\}$ is obtained by sampling at equal time intervals. The time scale is S. Then a time series $\left\{y_j^s\right\}$ related to the time length S is constructed after coarse-grained processing. The length is $1/S$ of the original sequence length, and the mean coarse-graining process is shown in **Fig. 3**.

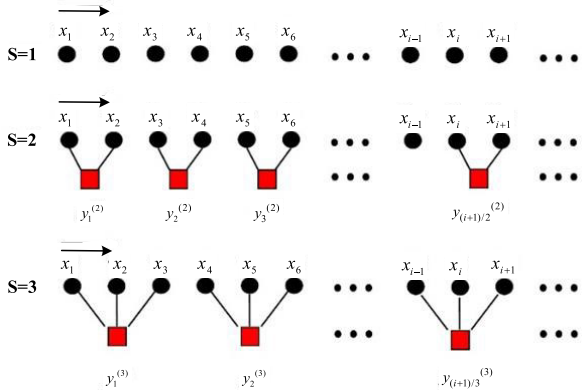

FIGURE 3. Schematic of the mean coarse-graining process.

The m-dimensional vector $X(1), X(2), \ldots, X(N\text{-}m+1)$ is reconstructed, where $X(i) = \left[x_1, x_2, x_3, \cdots, x_{(i+m-1)}\right]$. The similarity threshold is defined as r, and the value range of r is $r = 0.1\times$ std $\sim 0.25\times$ std. For $1 \le i \le N-m+1$, count the number of vectors with distances less than r, and calculate the ratio of this vectors to the total number of vector pairs, as shown in (8):

$$B_i^m(r) = \frac{(\text{number of } X(j) \text{ such that } d\left[X(i), X(j)\right] \le r)}{N-m}, \quad i \ne j \tag{8}$$

$d\,[X(i), X(j)]$ is the distance between two vectors, as shown in (9).

$$d\,[X(i), X(j)] = Max\,[|x(i+k) - x(j+k)|]\,, \quad i \neq j, \quad k \in [0, m-1], \quad j \in [1, N-m+1] \tag{9}$$

For the m-dimensional and $k = m+1$-dimensional reconstructed sequence vector, the average value $B^m(r)$ and $B^{m+1}(r)$ of all i values is found. Equation (10) can be obtained as [36], [37], [38]:

$$\begin{cases} B_m(r) = \dfrac{\sum_{i=1}^{N-m+1} B_i^m(r)}{N-m+1} \\ B_{m+1}(r) = \dfrac{\sum_{i=1}^{N-m+1} B_i^{m+1}(r)}{N-m+1} \end{cases} \tag{10}$$

Then, the sample entropy of this scale is shown in (11)

$$SampEn(m, r, N) = -ln\frac{B^{m+1}(r)}{B^m(r)} \tag{11}$$

The mean coarse-grained algorithm is improved. The time scale is assumed to be S, and a new sequence $\left\{z_j^S\right\}$ is derived according to (10). When $S = 1$, only one sequence can be obtained, which is the same as the original sequence; when $S > 1$, the length is N-m/S-1. The schematic of the process of improving the mean coarse-graining is shown in **Fig. 4**. The greatest improvement is the employment of overlapping sliding time windows to define the next time window by specifying the sliding step of each time window, so as to solve the problem of inaccurate analysis results caused by the sharp decrease of time series length.

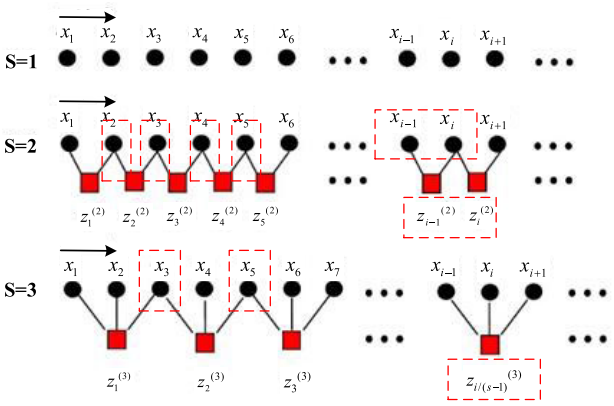

FIGURE 4. Schematic of the improved mean coarse-graining process.

After the sample entropy of the multiple sequences constructed at each scale is calculated, the mean value of the sample entropy of each scale is calculated, and the improved entropy value under this scale is obtained.

IV. RESULTS AND DISCUSSION

A. ANALYSIS OF EEG AMPLITUDE AND POWER SPECTRUM CHARACTERISTICS

1) EEG AMPLITUDE CHARACTERISTIC ANALYSIS

Many studies have shown that, under cognitive workload generated by different mathematical calculations, the frontal area of the human brain has the highest energy sensitivity and is more relatively concentrated. Therefore, the potential signal amplitude in the left and right frontal areas of the brain is used for research [39], [40], [41]. **Tables 2–5** show the mean value and standard deviation of the different waveband amplitudes in the driver's left and right frontal areas under normal driving conditions and different cognitive workloads.

TABLE 2. Characteristics of brain amplitude under normal driving.

Left Brain (μV)			Right Brain (μV)		
Waveband	Mean	SD	Waveband	Mean	SD
Delta	10.0885	3.9398	Delta	11.9725	4.8564
Theta	12.7406	9.1522	Theta	8.3759	5.7375
Alpha	17.2987	12.1809	Alpha	11.9257	8.9256
Beta	27.0125	13.3167	Beta	19.8702	13.3214
Gamma	48.9888	17.4890	Gamma	50.0663	26.1642

TABLE 3. Characteristics of brain amplitude under mild workload.

Left Brain (μV)			Right Brain (μV)		
Waveband	Mean	SD	Waveband	Mean	SD
Delta	18.6869	16.5512	Delta	21.1295	16.8320
Theta	21.0690	15.3377	Theta	17.5424	13.5968
Alpha	29.8617	24.3694	Alpha	29.0571	16.5577
Beta	66.0618	38.4453	Beta	63.3506	36.1217
Gamma	55.1394	33.3126	Gamma	44.0243	21.2094

TABLE 4. Characteristics of brain amplitude under moderate workload.

Left Brain (μV)			Right Brain (μV)		
Waveband	Mean	SD	Waveband	Mean	SD
Delta	32.0895	18.3655	Delta	25.5600	17.3310
Theta	28.1537	13.4124	Theta	21.8032	13.8071
Alpha	23.7485	16.9371	Alpha	40.2353	21.1401
Beta	67.5465	34.443	Beta	81.1638	51.6384
Gamma	69.4170	43.6126	Gamma	57.9037	29.4460

TABLE 5. Characteristics of brain amplitude under high workload.

Left Brain (μV)			Right Brain (μV)		
Waveband	Mean	SD	Waveband	Mean	SD
Delta	26.4880	21.3418	Delta	26.0882	22.2504
Theta	33.6412	22.7039	Theta	36.6912	25.8049
Alpha	38.5259	34.2463	Alpha	47.2646	40.0670
Beta	117.1852	66.9002	Beta	115.9584	70.4366
Gamma	83.1660	58.7471	Gamma	72.4631	49.1782

Tables 2–5 show that as the degree of cognitive workload deepens, the amplitude of each band gradually increases, but the amplitude is significantly different. Taken together, the delta, theta and alpha waves have relatively small amplitudes,

while the beta and gamma waves will have greater changes with different levels of cognitive workload.

For delta waves, the left brain gradually increases under light and moderate workloads but begins to decrease under high workloads; although the amplitude of the right brain increases with the depth of the workload, the changing trend is slow. Under normal driving conditions and mild cognitive workload, the amplitude of the right brain is higher than that of the left brain. Under moderate cognitive workload, the amplitude of the left brain is significantly higher than that of the right brain. Under high cognitive workload, the amplitudes of the left and right brains are basically the same.

For theta wave, the amplitude of the left brain and right brain gradually increases with the increase in the cognitive workload; in a normal driving state, the amplitude of the left brain is higher than that of the right brain under mild cognitive workload and moderate cognitive workload. Under high cognitive workload, the right brain is higher than the left brain.

For the alpha wave, the amplitude of the left brain starts to increase when the cognitive workload is mild, and it decreases when the cognitive workload is moderate and continues to increase when the cognitive workload is high. The amplitude of the right brain gradually increases with the increase in the level of cognitive workload; in the normal driving state, the amplitude of the left brain is higher than that of the right brain. When the cognitive workload is mild, the amplitude of the left and right brains is basically the same, but under moderate and high cognitive workload, the amplitude of the right brain is significantly higher than that of the left brain.

For the beta wave, compared with normal driving conditions, the left brain has a larger increase in mild cognitive workload, a weak increase in moderate cognitive workload and a larger increase in high cognitive workload. As the cognitive workload increases, the amplitude of the right brain continues to increase significantly. Under normal driving conditions and mild cognitive workload, the amplitude of the left brain is higher than that of the right brain. Under moderate cognitive workload, the amplitude of the right brain is higher than that of the left brain. Under high cognitive workload, the amplitude of the two is basically the same.

For the gamma waves, the amplitude of the left brain increased with the increase in cognitive workload. The right brain amplitude was lower during mild cognitive distraction than in normal driving and increased continuously under moderate and high cognitive workloads. The right brain amplitude is higher than the left brain amplitude under normal driving, moderate and high cognitive workload, and also under mild cognitive workload.

2) POWER SPECTRUM CHARACTERISTIC ANALYSIS

Fast waves and slow waves have different effects on the brain under different conditions. The EEG data collected in the experiment are analysed to calculate the average power spectral density of different frequency bands in the EEG signal to obtain the average power of different frequency bands. The ratio of density R (alpha/beta), R (delta/beta), R (theta/beta), R (gamma/alpha + beta), R (theta + delta/alpha + beta), delta and theta represent slow waves; alpha, beta and gamma represent fast waves; and these ratios can reflect the characteristic laws between slow waves, fast waves and fast-slow waves.

Figs. 5(a), **5(b)** and **5(c)** show the comparison among different bands to beta under different conditions. With the deepening of cognitive degree, the ratio of slow wave (delta and theta) to beta significantly decreased, and significant differences were found between the left and right brains. The differences between left and right brain possibly because that the left hemisphere controls people's action behaviors, such as language and calculations, while the right hemisphere controls people's imagination, spatial thinking, and intuitive feelings. Therefore, it shows differences between left and right brains. Under mild and moderate cognitive workloads, the ratio of the left brain was greater than that of the right brain, while the ratio of the right brain was in the left brain under high cognitive workload. Fast wave alpha/beta gradually decreased as cognitive workload deepened. No significant difference was found between the left and right brains during normal driving states and under mild cognitive workload, but the ratio of the right brain was slightly higher under moderate cognitive workload, while the ratio of the left brain was higher under high cognitive workload.

In the combined ratio, **Fig. 5(d)** shows the ratio between the sum of the two fast waves and the highest frequency gamma. The gamma/(alpha + beta) ratio is the highest under the normal driving state, and the ratio of the right brain is higher than that of the left brain. With the deepening of cognitive degree, the ratio decreases compared with that of the normal driving state, and the value of the left brain is higher than that of the right brain. With the deepening of cognitive workload, the left brain shows a trend of rising first and then falling, while the ratio of the right brain is relatively stable. **Fig. 5(e)** shows the ratio of the sum of the two slow waves to the sum of the two fast waves. Under the normal driving condition, this ratio was the highest in both the left and right brains, with the right brain being significantly greater than the left brain. When cognitive load appeared, this ratio decreased, with the left brain being the lowest under mild cognitive load and still lower than the right brain. With the deepening of cognitive workload, the left brain showed a trend of first rising and then declining, while the right brain showed a relatively stable performance.

B. IMPROVED MULTI-SCALE SAMPLE ENTROPY UNDER DIFFERENT COGNITIVE WORKLOADS

The 30 scales of the improved MSE and the traditional MSE of the normal driving state data are analysed, and the results are shown in **Fig. 6**.

A comparison among the entropy changes of the traditional MSE and the improved MSE at various scales shows that as the scale increases, all bands show a downward trend, but the changing trend of the improved algorithm is more obvious

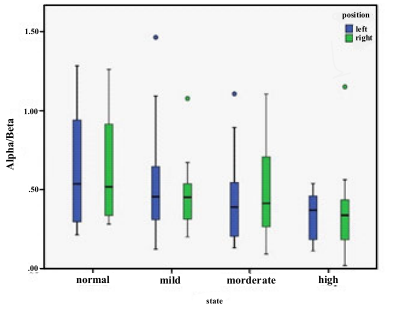

(a) Alpha/Beta

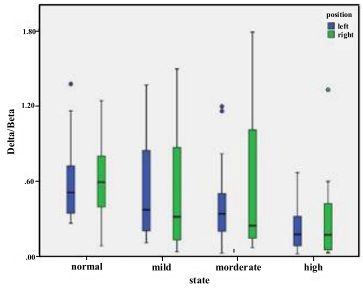

(b) Delta/Beta

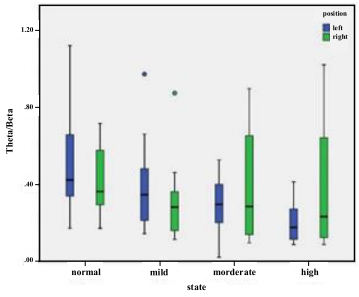

(c) Theta/Beta

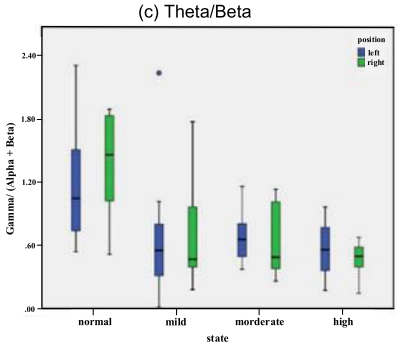

(d) Gamma/ (Alpha + Beta)

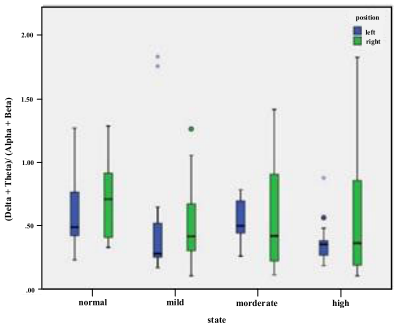

(e) (Delta + Theta)/ (Alpha + Beta)

FIGURE 5. Power spectrum ratio of each frequency band.

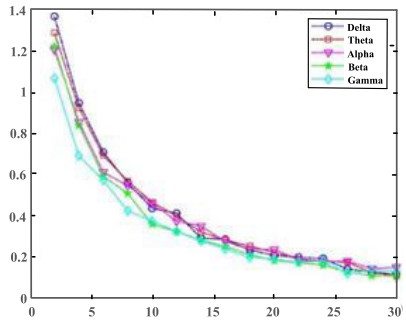

(a) Traditional MSE in normal driving

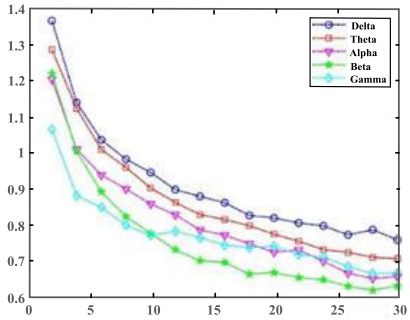

(b) Improved MSE in normal driving

FIGURE 6. Comparison of improved multi-scale sample entropy and traditional sample entropy under normal driving state.

among all bands, its entropy fluctuation range is smaller, and the complexity change degree is more objective. **Fig. 6(b)** shows that in normal driving conditions, the delta wave has the highest entropy value and is more complex, followed by the theta wave. The gamma wave has the lowest complexity when the scale factor is less than 10, but afterward, it is greater than 10, and its complexity gradually becomes higher than that of the beta wave.

Through an analysis of the improved MSE under different cognitive workload states, **Fig. 7** shows that the entropy of the theta wave is the highest and its complexity is greater under mild cognitive distraction. The complexity of gamma is the lowest at all scales, while the other three frequency bands show a gradual and alternating downward trend under different scale factors. The degree of complexity change of delta and alpha waves is basically the same after scale 10. Beta waves are similar in complexity to alpha waves within a scale factor of 5, but as the scale factor increases, their complexity decreases gradually. Under moderate cognitive workload, the entropy values of the five frequencies gradually decrease with the increase in the scale factor. The delta, theta and alpha waves have similar complexity, being at a more complex level, while the entropy of gamma is above that of beta, but its complexity is still relatively low. Under high cognitive workload, the entropy value of the gamma wave is the largest and significantly higher than that of other frequency bands, thereby indicating that the complexity effect of the gamma wave is the most obvious at this stage.

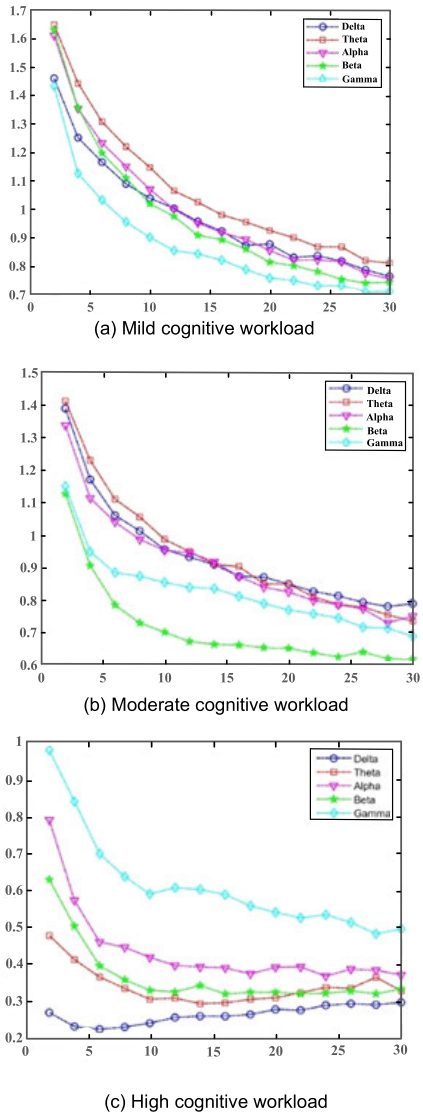

FIGURE 7. Comparison of improved multi-scale sample entropy under different cognitive workload states.

The entropy value of the delta wave is at the lowest level under all scale factors, indicating that its wave value characteristics do not change obviously at this stage. Alpha and beta waves have a significant downward trend within scale 10. After scale factor 10, the complexity of the other four waves, except the gamma wave, tends to be stable.

V. CONCLUSION

An analysis of the characteristics of the EEG amplitude of the left and right brain waves under different states shows that the amplitude of delta, theta and alpha waves was small, while beta and gamma waves showed great changes under different degrees of cognitive workloads. Compared with normal driving, the values of the five brain waves all increased, and the changes in the left and right brains were greatly different.

An analysis of the power spectrum characteristics of left and right brain waves under different states shows that with the deepening of cognitive workload, the ratios of slow wave (delta and theta), fast wave (alpha) and beta all showed significant decreases, but the performance of the left and right brains was different. In the study of the combined wave ratio, the values of the left brain (gamma/(alpha + beta) and (delta + theta)/(alpha + beta) showed a trend of first increasing and then decreasing with the deepening of cognitive degree, while the changes of the right brain were relatively stable in each stage. Compared with the normal driving state, these ratios all declined.

The improved multi-scale sample entropy algorithm has more obvious change trends between bands at different stages, its entropy fluctuation range is smaller and the degree of complexity change is more objective. In a normal driving state, the entropy value of the delta wave is the largest, and as the scale increases, the entropy value decreases. Under mild cognitive workload, the entropy value of theta is always the largest, and the entropy value of gamma is the lowest. With the increase in the scale factor, the entropy value decreases. Under moderate cognitive workload, as the scale factor increases, the entropy values of alpha, theta and delta alternately lead, but the entropy values of gamma and beta are always low. As the scale factor increases, the entropy value shows a decreasing trend. Under high cognitive workload, the entropy value of gamma is always the largest, followed by alpha, and the entropy value of delta is always at the lowest level. After the scale factor of 10, the complexity of the other four waves, except the gamma wave, tends to be stable.

VI. LIMITATION AND FUTURE WORK

The rules of EEG characteristics under different states in this paper do not consider the difference between the driving simulation and the actual driving experiment. Besides, due to the complexity of implementing the experiments as well as other project constraints (complexity of experiment implementation, funding), there were several limitations to this study. More participants will be recruited to explore the brain characteristics of drivers under cognitive workload, and we will add some driving simulation experiments for supplementary comparative analysis.

In this paper, continuous wavelet decomposition is adopted for signal noise processing and waveform decomposition. In future research, white noise and other filters will be added for signal denoising, and waveform decomposition will be conducted in other ways. We will further study the difference between left and right brains, as well as the resource occupancy trends of the monitor, perception, visual and auditory channels in different driving conditions.

ACKNOWLEDGMENT

The authors acknowledge the anonymous reviewers for their valuable comments and suggestions.

REFERENCES

[1] *Overview of Motor Vehicle Crashes in 2019*, Nat. Center Statist. Anal., Traffic Saf. Facts Res. Note., Tech. Rep. DOT HS 813 060, Dec. 2020.

[2] H. Berge, "On the electroencephalogram of man. Sixth report," *Electroencephalogr. Clin. Neurophysiol. Suppl.*, vol. 28, p. 173, Jan. 1969.
[3] J. L. O'Leary, "Book reviews: Discoverer of the brain wave," *Science*, vol. 168, pp. 562–563, May 1970.
[4] M. E. Raichle, "Two views of brain function," *Trends Cognit. Sci.*, vol. 14, no. 4, pp. 180–190, Apr. 2010.
[5] J. D. Cohen, S. D. Forman, T. S. Braver, B. J. Casey, D. Servan-Schreiber, and D. C. Noll, "Activation of the prefrontal cortex in a nonspatial working memory task with functional MRI," *Hum. Brain Mapping*, vol. 1, no. 4, pp. 293–304, Jun. 1994.
[6] J. Kong, C. Wang, K. Kwong, M. Vangel, E. Chua, and R. Gollub, "The neural substrate of arithmetic operations and procedure complexity," *Cognit. Brain Res.*, vol. 22, no. 3, pp. 397–405, Mar. 2005.
[7] H. Kou and S. Iwaki, "Modulation of neural activities by the complexity of mental arithmetic: An MEG study," *Int. Congr. Ser.*, vol. 1300, pp. 539–542, Jun. 2007.
[8] S. Aydın, Ç. Güdücü, F. Kutluk, A. Öniz, and M. Özgören, "The impact of musical experience on neural sound encoding performance," *Neurosci. Lett.*, vol. 694, pp. 124–128, Feb. 2019.
[9] M. Lohani, B. R. Payne, and D. L. Strayer, "A review of psychophysiological measures to assess cognitive states in real-world driving," *Frontiers Hum. Neurosci.*, vol. 13, p. 57, Mar. 2019.
[10] F. M. Al-Shargie, O. Hassanin, U. Tariq, and H. Al-Nashash, "EEG-based semantic vigilance level classification using directed connectivity patterns and graph theory analysis," *IEEE Access*, vol. 8, pp. 115941–115956, 2020.
[11] W. Zeng, M. Li, C. Yuan, Q. Wang, F. Liu, and Y. Wang, "Identification of epileptic seizures in EEG signals using time-scale decomposition (ITD), discrete wavelet transform (DWT), phase space reconstruction (PSR) and neural networks," *Artif. Intell. Rev.*, vol. 53, no. 4, pp. 3059–3088, Apr. 2020.
[12] S. Khessiba, A. G. Blaiech, K. B. Khalifa, A. B. Abdallah, and M. H. Bedoui, "Innovative deep learning models for EEG-based vigilance detection," *Neural Comput. Appl.*, vol. 33, no. 12, pp. 6921–6937, Jun. 2021.
[13] Z. Gao, X. Wang, Y. Yang, C. Mu, Q. Cai, W. Dang, and S. Zuo, "EEG-based spatio–temporal convolutional neural network for driver fatigue evaluation," *IEEE Trans. Neural Netw. Learn. Syst.*, vol. 30, no. 9, pp. 2755–2763, Sep. 2019.
[14] S. Kar, M. Bhagat, and A. Routray, "EEG signal analysis for the assessment and quantification of driver's fatigue," *Transp. Res. F, Traffic Psychol. Behav.*, vol. 13, no. 5, pp. 297–306, Sep. 2010.
[15] R. Mahmoud, T. Shanableh, I. P. Bodala, N. V. Thakor, and H. Al-Nashash, "Novel classification system for classifying cognitive workload levels under vague visual stimulation," *IEEE Sensors J.*, vol. 17, no. 21, pp. 7019–7028, Nov. 2017.
[16] Y. Jiao, Y. Deng, Y. Luo, and B.-L. Lu, "Driver sleepiness detection from EEG and EOG signals using GAN and LSTM networks," *Neurocomputing*, vol. 408, pp. 100–111, Sep. 2020.
[17] B. T. Jap, S. Lal, and P. Fischer, "Comparing combinations of EEG activity in train drivers during monotonous driving," *Expert Syst. Appl.*, vol. 38, no. 1, pp. 996–1003, Jan. 2011.
[18] C.-T. Lin, S.-A. Chen, T.-T. Chiu, H.-Z. Lin, and L.-W. Ko, "Spatial and temporal EEG dynamics of dual-task driving performance," *J. Neuroeng. Rehabil.*, vol. 8, no. 1, pp. 1–13, Feb. 2011.
[19] G. Borghini, L. Astolfi, G. Vecchiato, D. Mattia, and F. Babiloni, "Measuring neurophysiological signals in aircraft pilots and car drivers for the assessment of mental workload, fatigue and drowsiness," *Neurosci. Biobehav. Rev.*, vol. 44, pp. 58–75, Jul. 2014.
[20] Y. Fan, L.-L. Zeng, H. Shen, J. Qin, F. Li, and D. Hu, "Lifespan development of the human brain revealed by large-scale network eigen-entropy," *Entropy*, vol. 19, no. 9, p. 471, Sep. 2017.
[21] L. Montesinos, R. Castaldo, and L. Pecchia, "On the use of approximate entropy and sample entropy with centre of pressure time-series," *J. Neuroeng. Rehabil.*, vol. 15, no. 1, pp. 1–15, Dec. 2018.
[22] J. Olbrys and E. Majewska, "Approximate entropy and sample entropy algorithms in financial time series analyses," *Proc. Comput. Sci.*, vol. 207, pp. 255–264, Oct. 2022.
[23] C. Li and P. Shang, "Multiscale tsallis permutation entropy analysis for complex physiological time series," *Phys. A, Stat. Mech. Appl.*, vol. 523, pp. 10–20, Jun. 2019.
[24] S.-F. Liang, Y.-H. Kuo, Y.-H. Hu, Y.-H. Pan, and Y.-H. Wang, "Automatic stage scoring of single-channel sleep EEG by using multiscale entropy and autoregressive models," *IEEE Trans. Instrum. Meas.*, vol. 61, no. 6, pp. 1649–1657, Jun. 2012.
[25] C. A. C. Ortega, M. A. Mariscal, W. Boulagouas, S. Herrera, J. M. Espinosa, and S. García-Herrero, "Effects of mobile phone use on driving performance: An experimental study of workload and traffic violations," *Int. J. Environ. Res. Public Health*, vol. 18, no. 13, p. 7101, Jul. 2021.
[26] A. Humeau-Heurtier, "Multivariate generalized multiscale entropy analysis," *Entropy*, vol. 18, no. 11, p. 411, Nov. 2016.
[27] Y. Liu, Y. Lin, J. Wang, and P. Shang, "Refined generalized multiscale entropy analysis for physiological signals," *Phys. A, Stat. Mech. Appl.*, vol. 490, pp. 975–985, Jan. 2018.
[28] S. Aydin, N. Arica, E. Ergul, and O. Tan, "Classification of obsessive compulsive disorder by EEG complexity and hemispheric dependency measurements," *Int. J. Neural Syst.*, vol. 25, no. 3, Mar. 2015, Art. no. 1550010.
[29] M. U. Ahmed and D. P. Mandic, "Multivariate multiscale entropy analysis," *IEEE Signal Process. Lett.*, vol. 19, no. 2, pp. 91–94, Feb. 2012.
[30] M. Hu and H. Liang, "Variance entropy: A method for characterizing perceptual awareness of visual stimulus," *Appl. Soft Comput.*, vol. 2012, Jan. 2012, Art. no. 525396.
[31] M. D. Costa and A. L. Goldberger, "Generalized multiscale entropy analysis: Application to quantifying the complex volatility of human heartbeat time series," *Entropy*, vol. 17, no. 3, pp. 1197–1203, Mar. 2015.
[32] A. Khanna, A. Pascual-Leone, C. M. Michel, and F. Farzan, "Microstates in resting-state EEG: Current status and future directions," *Neurosci. Biobehav. Rev.*, vol. 49, pp. 105–113, Feb. 2015.
[33] J. Stapel, F. A. Mullakkal-Babu, and R. Happee, "Automated driving reduces perceived workload, but monitoring causes higher cognitive load than manual driving," *Transp. Res. F, Traffic Psychol. Behav.*, vol. 60, pp. 590–605, Jan. 2019.
[34] P. Biswas and G. Prabhakar, "Detecting drivers' cognitive load from saccadic intrusion," *Transp. Res. F, Traffic Psychol. Behav.*, vol. 54, pp. 63–78, Apr. 2018.
[35] C. Ahlstrom and K. Kircher, "Changes in glance behaviour when using a visual eco-driving system—A field study," *Appl. Ergonom.*, vol. 58, pp. 414–423, Jan. 2017.
[36] N. Zhang, A. Lin, H. Ma, P. Shang, and P. Yang, "Weighted multivariate composite multiscale sample entropy analysis for the complexity of nonlinear times series," *Phys. A, Stat. Mech. Appl.*, vol. 508, pp. 595–607, Oct. 2018.
[37] M. Xu and P. Shang, "Analysis of financial time series using multiscale entropy based on skewness and kurtosis," *Phys. A, Stat. Mech. Appl.*, vol. 490, pp. 1543–1550, Jan. 2018.
[38] Y. Yin, X. Wang, Q. Li, and P. Shang, "Generalized multivariate multiscale sample entropy for detecting the complexity in complex systems," *Phys. A, Stat. Mech. Appl.*, vol. 545, May 2020, Art. no. 123814.
[39] R. Ishii, L. Canuet, T. Ishihara, Y. Aoki, S. Ikeda, M. Hata, T. Katsimichas, A. Gunji, H. Takahashi, T. Nakahachi, M. Iwase, and M. Takeda, "Frontal midline theta rhythm and gamma power changes during focused attention on mental calculation: An MEG beamformer analysis," *Frontiers Hum. Neurosci.*, vol. 8, pp. 1–10, Jun. 2014.
[40] P. W. Burgess, N. Alderman, E. Volle, R. G. Benoit, and S. J. Gilbert, "Mesulam's frontal lobe mystery re-examined," *Restorative Neurol. Neurosci.*, vol. 27, no. 5, pp. 493–506, Oct. 2009.
[41] M. J. Vansteensel, M. G. Bleichner, Z. V. Freudenburg, D. Hermes, E. J. Aarnoutse, F. S. S. Leijten, C. H. Ferrier, J. M. Jansma, and N. F. Ramsey, "Spatiotemporal characteristics of electrocortical brain activity during mental calculation," *Hum. Brain Mapping*, vol. 35, no. 12, pp. 5903–5920, Dec. 2014.

RUIWEI LIU was born in Bengbu, Anhui, China, in 1991. He received the Ph.D. degree from the Harbin Institute of Technology, Harbin, China, in 2020. He is currently a Lecturer with the School of Naval Architecture and Ocean Engineering, Guangzhou Maritime University, China. His research interests include cable-driven robot, tensegrity robot, and space-deployable structure and control.

SHOUMING QI received the Ph.D. degree in transportation planning and management from the Harbin Institute of Technology at Shenzhen. He was a Visiting Scholar with the University of California, Berkeley (UCB). His research interests include transportation safety and human factors.

SIQI HAO was born in Siping, Jilin, China, in 1990. She received the Ph.D. degree from the Harbin Institute of Technology, Harbin, China, in 2020. She is currently a Lecturer with the School of Naval Architecture and Ocean Engineering, Guangzhou Maritime University, China. Her research interest includes transportation safety and control.

GUAN LIAN received the Ph.D. degree in transportation planning and management from the Harbin Institute of Technology, in 2019. He is currently an Associate Professor with the Guilin University of Electronic Technology. His current research interest includes the application of data mining technology in urban transportation.

YINGTONG LI is currently pursuing the bachelor's degree with the Department of Ports and Shipping Management, Guangzhou Maritime University. Her current research interests include human factors, and transportation safety and control.

HAIHUA YANG received the Ph.D. degree in transportation planning and management from the Harbin Institute of Technology. He was a Visiting Scholar with The Hong Kong Polytechnic University. His research interest includes transportation network modeling and analysis.